Multidimensional analysis of the frequencies and rates of cytokine secretion from single cells by quantitative microengraving

Citation: Han, Qing, Elizabeth M. Bradshaw, Björn Nilsson, David A. Hafler, and J. Christopher Love. Multidimensional Analysis of the Frequencies and Rates of Cytokine Secretion from Single Cells by Quantitative Microengraving. Lab on a Chip 10, no. 11 (2010): 1391.

As Published: http://dx.doi.org/10.1039/b926849a

Publisher: Royal Society of Chemistry

Persistent URL: http://hdl.handle.net/1721.1/79379

Version: Author's final manuscript: final author's manuscript post peer review, without publisher's formatting or copy editing

Published in final edited form as:
Lab Chip. 2010 June 7; 10(11): 1391–1400. doi:10.1039/b926849a.

Multidimensional analysis of the frequencies and rates of cytokine secretion from single cells by quantitative microengraving

Qing Han[a], **Elizabeth M. Bradshaw**[b], **Björn Nilsson**[c], **David A. Hafler**[c,d], and **J. Christopher Love**[*,a,c]

[a] Department of Chemical Engineering, Massachusetts Institute of Technology, 77 Massachusetts Ave., Cambridge, MA 02139

[b] Division of Molecular Immunology, Center for Neurologic Diseases, Brigham and Women's Hospital, Harvard Medical School, 77 Avenue Louis Pasteur, Boston, MA 02115

[c] The Eli and Edythe L. Broad Institute, Seven Cambridge Center, Cambridge, MA 02139

[d] Department of Neurology, Yale University, 15 York Street, P.O. Box 208018, New Haven, CT 06520

Summary

The large diversity of cells that comprise the human immune system requires methods that can resolve the individual contributions of specific subsets to an immunological response. Microengraving is process that uses a dense, elastomeric array of microwells to generate microarrays of proteins secreted from large numbers of individual live cells (~10^4–10^5 cells/assay). In this paper, we describe an approach based on this technology to quantify the rates of secretion from single immune cells. Numerical simulations of the microengraving process indicated an operating regime between 30 min-4 h that permits quantitative analysis of the rates of secretion. Through experimental validation, we demonstrate that microengraving can provide quantitative measurements of both the frequencies and the distribution in rates of secretion for up to four cytokines simultaneously released from individual viable primary immune cells. The experimental limits of detection ranged from 0.5 to 4 molecules/s for IL-6, IL-17, IFNγ, IL-2, and TNFα. These multidimensional measures resolve the number and intensities of responses by cells exposed to stimuli with greater sensitivity than single-parameter assays for cytokine release. We show that cells from different donors exhibit distinct responses based on both the frequency and magnitude of cytokine secretion when stimulated under different activating conditions. Primary T cells with specific profiles of secretion can also be recovered after microengraving for subsequent expansion *in vitro*. These examples demonstrate the utility of quantitative, multidimensional profiles of single cells for analyzing the diversity and dynamics of immune responses in vitro and for identifying rare cells from clinical samples.

Introduction

Identifying clinical markers that correlate with a protective response to a vaccine or that indicate the efficacy of a treatment for a disease remains a significant challenge. Distinct functional responses, such as the secretion of one or more cytokines or the proliferative

[*]Correspondence should be addressed to: J. Christopher Love, Ph.D., Department of Chemical Engineering, Massachusetts Institute of Technology, 77 Massachusetts Ave., Bldg. 66-456, Cambridge, MA 02139, Phone: 617-324-2300, Fax: 617-258-5042, clove@mit.edu.

capacity of a cell, can distinguish unique subsets of lymphocytes that may be associated with the quality of an immune response.[1] Resolving heterogeneities among subsets of cells would be aided, however, by analytical methods that yield multiple measures of the breadth and quality of functions exhibited by individual lymphocytes.[2]

Existing analytical methods can assess the frequencies, magnitude, and number of cytokines produced by individual cells, but not in a comprehensive manner. That is, there are few if any assays that assign multiple functional and phenotypic characteristics to the same individual cells without affecting their viability or responses, or requiring surrogate markers for their activity. Enzyme-linked immunospot (ELISpot) assays are a common method for measuring the frequencies of primary immune cells producing specific proteins such as cytokines after stimulation *in vitro*.[3] The technique relies on capturing secreted proteins using high-affinity antibodies immobilized on a surface close to individual secreting cells and subsequent detection by a colorimetric, enzymatic reaction. Quantifying the subtle differences among responding cells within a population is difficult, however, for several reasons: 1) individual spots vary in size and may overlap; 2) these assays typically require extended incubations over 12–48 h to detect cytokine-secreting cells, thus limiting the temporal resolution of responses; 3) conventional colorimetric detection restricts the number of concurrent proteins detected; and 4) the cells are lost during the process, thereby hindering further phenotypic analyses. The use of fluorescently-labeled antibodies has expanded the number of secreted factors that can be detected simultaneously,[4–6] but these modifications have not decreased the minimum time required to detect secreted cytokines (6–18 h). For antibody-secreting cells (ASCs), the intensities of spots generated in colorimetric and fluorescent ELISpots have been used to assign rates of secretion after long periods of incubation.[7, 8] Whether these approaches can be used to determine the rates of secreted cytokines is not clear: ASCs produce significantly more protein than most cytokine-secreting cells ($\ll$100 molecules/s), and the standards used for comparison in the colorimetric assays are highly non-linear within the range of detection most relevant for cytokines.

The combination of intracellular staining (ICS) and multiparameter cytometry has become a common alternative to assess the number and magnitude of cytokines expressed by single cells.[9, 10] Cells are stimulated for 4–6 h in the presence of inhibitors that block secretion, and then fixed, permeated, and labeled with antibodies specific for the accumulated intracellular proteins of interest. Mean fluorescence intensities (MFI) of these labels measured by flow cytometry or imaging cytometry provide a relative measure of the quantity of a protein trapped intracellularly.[11, 12] Using these values to quantify expression is challenging, as there is not a suitable standard for converting the measured values into precisely quantifiable amounts of cytokine. Thus, it is difficult to compare the magnitude of responses directly among independent samples. Furthermore, ICS measures only the productive capacity of a cell when prohibited from secretion. This imposed perturbation may alter the responses of the cells and may not accurately reflect the quantities of cytokine that would have been secreted by the cell.[13] Two modified approaches for flow cytometry—'artificial receptors' and microbeads[14–16]–allow the capture of secreted cytokines near the extracellular surface of the cell. Analytical models for the mass transport in these two processes indicate, however, that the rate of diffusion of released cytokines into the bulk media limits the sensitivity of these measurements for poor secretors and may introduce cross-contamination among cells.[17] Encapsulation of cells at cold temperatures in polymeric matrices may also perturb secretion, and requires additional processing to recover them.

Analytical tools for fast (< 6 h) and multiplexed determination of secreted proteins from live primary cells would help resolve the dynamic behaviors of individual cells following stimulation, and minimize external perturbations that could unintentionally alter their

behaviors. Arrays of microwells have been manufactured using a range of materials to facilitate the isolation and interrogation of single cells.[18–27] We previously developed a technique, called microengraving, that uses an elastomeric array of microfabricated wells to confine individual viable cells temporarily in subnanoliter volumes, and subsequently, to generate microarrays of proteins secreted from each cell.[28–31] A glass substrate defines one internal surface of the volumes, and supports an antibody to capture specific proteins secreted from the cell (Fig. 1a and Fig. S1). After incubation, the glass bearing captured proteins is removed and interrogated by applying fluorescent antibodies. This process has made it possible to measure the frequency of cells secreting specific proteins after short periods of incubation (~3–120 min). Release of proteins over time into the small volumes of media (~100 pL) surrounding each confined cell allows the sensitive detection of even poor secretors, such as primary cytokine-secreting cells. The steady accumulation of protein on the surface over time during this process suggested that it should be possible to calculate the average rates of secretion for each cell. Here, we used numerical simulations to determine the optimal ranges of conditions for quantifying protein captured from individual cells, and then, show quantification of the rates of secretion for as many as four cytokines in parallel for ~10^4–10^5 single primary human lymphocytes. This additional analytical dimension improves the distinctions between responses induced in primary lymphocytes following stimulations *in vitro* by assigning both a frequency and magnitude to responding cells. To further demonstrate the utility of this system for integrative single-cell analysis, we also show that measuring specific secretory profiles can guide the identification and retrieval of T cells for expansion *in vitro*.

Mathematical model

To analyze the dynamics of capturing analytes during microengraving, we developed a numerical model that accounts for the secretion of proteins from cells, the diffusion of those proteins in a confined volume, and the binding of those proteins onto a surface bearing antibodies with specific affinities for the secreted analytes. The model describes a single cell confined in a cubic container (50 μm in each linear dimension) that comprises a bottom and four sidewalls manufactured in poly(dimethylsiloxane) (PDMS) and a top defined by a glass surface. In the simplest embodiment of the model, the glass surface forming the top of the reactor supports capture antibodies specific for only one analyte (Fig. 1a).

We made three assumptions that simplified the model and subsequent numerical simulations. First, the transport of analytes in the media results only from diffusion because there is no active flow or exchange of fluids in the sealed microwells during incubation. Second, we assumed that the PDMS walls were impermeable to analyte and that the adsorption of analyte on these surfaces contributed negligibly to the capture of proteins. For microengraving, the PDMS is typically treated with a buffered solution containing bovine serum albumin (BSA) or culture media with 10% bovine serum prior to depositing cells into the wells.[32] These treatments may not eliminate non-specific adsorption completely, but non-specific capture on BSA/serum-treated PDMS should be significantly lower than the specific capture on the glass slide. We, therefore, considered this interaction to be negligible in the model. Finally, we assumed proteins were secreted from the cell at a constant rate (κ). The total quantity of protein released from the cell in the volume of the reactor, therefore, increases monotonically with time:

$$N_{\text{total}} = \kappa t \tag{1}$$

where N_{total} is the total number of molecules secreted from the cell, κ is the rate of secretion, and t is the incubation time. The rate of secretion for a live cell likely fluctuates somewhat in

time depending on extrinsic factors such as the quality of its environment as well as intrinsic factors such as its secretory capacity and its state in the cell cycle.[33] Nevertheless, the assumption of a constant rate in this model is useful for understanding the relationship between the amount of protein secreted and the amount captured on the glass surface at any point in time.

The model comprises two equations that describe the diffusion of proteins from the secreting cell and their capture onto the functionalized surface. The equation for the diffusion of protein inside the volume of a closed well is:

$$\frac{\partial C}{\partial t} - D\nabla^2 C = 0 \tag{2}$$

where C is the concentration of analyte in the media and D is the diffusion coefficient of analyte. The reaction of the secreted analyte with the capture antibody supported on the glass surface is described by a reversible process:

$$\text{Analyte} + \text{Ab} \underset{k_{\text{off}}}{\overset{k_{\text{on}}}{\rightleftharpoons}} \text{Analyte} \cdot \text{Ab}$$

The boundary condition describing the dynamics of adsorption and desorption of the proteins on the glass surface, therefore, is:

$$\frac{\partial C}{\partial t} = -k_{\text{on}} \cdot C \cdot (\theta_0 - C_s) + k_{\text{off}} \cdot C_s \tag{3}$$

where k_{on} is the rate of association, k_{off} is the rate of dissociation, C_s is the concentration of analyte:antibody complex on the glass surface, θ_0 is the density of total binding sites on the surface. θ_0-C_s describes the density of remaining binding sites available on the surface. In the experimental protocols for microengraving, the surface of an array of microwells containing cells is rinsed with fresh media immediately before sealing the array against the glass slide. This process dilutes the volume of each well by > 10^5 fold. Therefore, we assume the concentrations of protein both in solution and on the surface are initially negligible (C=0, C_s=0, and θ=θ_0 at t=0).

The parameters describing the biophysical properties of the cells and the proteins of interest were determined from typical values reported in the literature. Lymphocytes range in diameter from ~5 μm to 20 μm, and proteins of interest (cytokines ~ 15–45 kDa and antibodies ~ 150 kDa) exhibit diffusion coefficients of 10^{-9}–10^{-11} m^2/s.[17, 34] In this model, we fixed the diameter of the cell and the diffusion coefficient of the analyte (D) to 10 μm and 10^{-10} m^2/s, respectively. For the binding affinity of the antibody and the rate of secretion, we tested a range of different values in the model based on similar values reported previously in the literature.[17, 35, 36] The values of parameters used in the simulations described here are listed in Table 1.

Experimental

Numerical simulations

COMSOL Multiphysics 3.3 (COMSOL AB. Stockholm, Sweden) was used to solve the partial differential equations relating the secretion, diffusion, and binding of analytes with a specific capture antibody.

Preparation of poly-L-lysine slides

Poly-L-lysine slides were prepared according to published protocols available online (http://cat.ucsf.edu/pdfs/PolylysineSlides.pdf). Briefly, 3″×1″ glass slides (Corning) were cleaned in 2.5 M NaOH in 60% ethanol for 2 h. After thoroughly washing with deionized water, slides were submerged in 0.001% poly-L-lysine solution (diluted in 0.1×PBS) for 1 h. Coated slides were further washed with water, dried, and stored in a desiccator until use.

Immobilization of capture antibodies

Antibodies for capturing secreted proteins were diluted in a buffer comprising 50 mM sodium borate, 8 mM sucrose, and 50 mM NaCl (pH 9.0) to a final concentration of 10–50 μg/mL, and deposited on the surface of poly-L-lysine slides for at least 1 h at 25 °C. Slides were then placed in non-fat milk (3% w/v in PBS) for 30 min at 25 °C, washed three times with PBS, dipped in water, and spun dry.

Estimation of the available binding sites on glass

To estimate the number of binding sites available on a glass slide after adsorbing a capture antibody from solution, we used a fluorescent, sandwich-style assay to evaluate the saturating quantity of analyte immobilized on the surface. Briefly, a capture antibody (50 μg/mL) was spotted on the surface of poly-L-lysine slides (1 μL/spot) and incubated for 1 h at 25 °C. After blocking and washing the surface, the slide was placed in a 96-well Microplate Microarray Hardware (ArrayIt, MMH96) and 100 μL of recombinant antigen (100 ng/mL; e.g., IFNγ) was added on each spot. The dose was selected to saturate the capture antibody fully, as determined by serial dilution on similar arrays. After a 2 h incubation at 37 °C, the slide was washed, and a fluorescently labeled detection antibody (10μg/mL) was applied at 25°C. The labeled slide was then scanned, and the amount of detection antibody was calculated by comparison with data collected from a standard slide on which known amounts of the detection antibody were spotted. This experiment yielded an order-of-magnitude estimate of the number of binding sites available on the glass.

Microengraving

The experiments were performed as previously described with some modifications as noted.[28, 29] Briefly, an array of microwells was manufactured by injecting a silicone elastomer (polydimethylsiloxane, PDMS; 10:1 base:catalyst; Dow Corning) into a custom-built mold and cured at 80 °C for 1 h. The arrays were 1 mm thick and adhered directly to a 3″×1″ glass slide. Each array consisted of 72×24 blocks that each contained a 7×7 array of microwells (50 μm × 50 μm × 50 μm, with a center-to-center distance of 100 μm).[32] After exposing an array to an oxygen plasma for 30 s (Harrick PDC-32G), a cell suspension (~2×10^5/mL) was placed on the surface of the array, and the cells were allowed to settle into the wells by gravity at a density of ~1 cell per well (Fig. S1). After washing excess cells from the surface of the array with serum-free media, the loaded device was then placed onto a glass slide coated with capture antibodies. The combination of the array and glass slide was held together under sufficient compression in a hybridization chamber (Agilent Technologies, G2534A) to avoid leakage or contamination between wells[32] and incubated at 37 °C with 5% CO_2. After incubation, the glass slide was separated from the array and placed in PBS.

Analysis of printed microarrays

After microengraving, slides were incubated with 1% non-fat milk in PBST (PBS with 0.05% (v/v) Tween 20) for 15 min, washed three times with PBST, and then incubated with fluorescent antibodies (1 μg/mL) for 45 min at 25 °C. Finally, the slides were washed with PBST and PBS three times each, rinsed briefly with water, and spun dry. Reference slides

were made at the end of each experiment with the same detection antibodies used on the printed slides. Antibodies were diluted in water and spotted onto blank poly-L-lysine slides (1 μL/spot). The reference slides then were dried under vacuum. Slides probed with fluorescent dye and reference slides were scanned using a Genepix 4200AL microarray scanner (Molecular Devices). The accompanying commercial software (Genepix Pro 6.1) was used to extract the MFI of each spot. These data were filtered to remove spots that contained saturated pixels (%Sat. > 0) or that exhibited a high degree of covariance (CV > 60).

Hybridoma culture and IgG detection

Hybridoma cells HYB 099-01 (Anti-ovalbumin, Statens Serum Institute) were cultured at 37 °C in a 5% CO_2 incubator in DMEM Media (Mediatech) supplemented with 10% FBS (PAA Laboratories), 100 U/mL penicillin, 100 mg/mL streptomycin, 10 mM HEPES, 50 μM 2-mercaptoethanol, 1 mM sodium pyruvate and 0.1 mM nonessential amino acids. The cultures were split every 2–3 days to maintain a density of 10^5–10^6 cells/mL. Poly-L-lysine-coated glass slides were coated with a mixture of two secondary antibodies: goat anti-mouse IgG from Zymed (81-6500) and Southern Biotech (1010-01), 50 μg/mL of each. Three arrays of microwells were loaded with hybridoma cells from the same culture and used for microengraving for 15, 30, and 45 min. After microengraving, live cells were stained by adding 1 μM of Calcein violet AM (Invitrogen) on top of the microwells for 20 min; exposure to light was minimized during this step. The arrays of cells were then imaged. The antibodies captured on the glass slides were labeled with ovalbumin-Alexa 555 (Invitrogen, 2 μg/mL).

Human peripheral blood mononuclear cells (PBMCs) isolation and stimulation

Venous blood was drawn from healthy controls into green-capped, lithium heparin tubes (Kendall) with institutional Internal Review Board Approval. PBMCs were separated using density centrifugation on Ficoll-Paque PLUS (GE Healthcare). PBMCs were frozen at a concentration of $1–2\times10^7$/mL in 10% dimethylsulfoxide (Sigma-Aldrich)/90% fetal calf serum (Atlanta Biologicals). After thawing, the PBMCs were washed in PBS and resuspended at 10^6/mL in RPMI 1640 medium (Mediatech), supplemented with 10% FBS, 2 mM L-glutamine, 10 mM HEPES, 100 U/mL penicillin, 100 mg/mL streptomycin, 0.1 mM non-essential amino acids, and 1 mM sodium pyruvate. To stimulate IL-6 secretion, lipopolysaccharide (LPS) (10 μg/mL), phytohemagglutinin (PHA) (5 μg/mL), or pokeweed mitogen (PWM) (5 μg/mL) was added to cells in round bottom 96-well microtiter plates and then incubated at 37 °C with 5% CO_2. To detect IL-17, IFNγ, IL-2, and TNFα, cells were stimulated by phorbol 12-myristate 13-acetate (PMA) (10 ng/mL) and ionomycin (1 μg/mL) for 6 h.

IL-6 detection from PBMCs

Poly-L-lysine slides were coated with 40 μg/mL mouse anti-human IL-6 (MAB206, R&D) and 10 μg/mL goat anti-human IgG (81-7100, Invitrogen). Human PBMCs were stained with Calcein violet AM before loading onto the array. After depositing cells onto the array, the cells were imaged by automated epifluorescent microscopy under temperature and CO_2 control. During image collection, stimuli were included in the media and the array of wells was covered with a Lifterslip (Electron Microscopy Sciences). The array of wells was then rinsed gently with media containing a trace amount of human serum (1:40,000) (to label the locations of all microwells with human Ig) and immediately applied onto a glass slide pre-coated with capture antibodies for 2 h. A portion of the cells used in these experiments were also stimulated in bulk, and then collected for mRNA quantification by real-time PCR at intervals matched to the microengraving. Alexa Fluor 488 (A20000, Invitrogen) labeled goat anti-human IL-6 (AF-206-NA, R&D) and Alexa Fluor 700 (A20010, Invitrogen) labeled

goat anti-human IgG (109-175-098, Jackson Immune Research) were used for detection. To assess surface-expressed markers present on the cells after microengraving, 10 μg/ml of CD3-Alexa Fluor 488, CD11b-Alexa Fluor 568, and CD14-Alexa Fluor 660 were added on the array of wells. After 30 min incubation in 4°C, the array of wells was washed by PBS and re-imaged.

Real-time PCR

RNA from PBMCs was purified using the absolutely RNA microprep kit (Stratagene). cDNA was made using a Taqman kit with supplied random hexamers (Applied Biosystems). The *β2-microglobulin* (*B2M*) and *IL-6* primers and probe were obtained from Applied Biosystems and used according to recommended methodologies. The *IL-6* gene expression is shown relative to *B2M*.

Multiplexed detection of cytokines

Pairs of antibodies used for multiplex cytokine detection were: IFNγ (MABTECH), IL-17 (eBioscience), IL-2 (R&D), and TNFα (BD). All the detection antibodies were labeled by Alexa Fluor-NHS esters according to manufacturer's instructions (Invitrogen). For capture, 10 μg/ml of each capture antibody was used to coat the poly-L-lysine slides. PBMCs were stained with Calcein violet AM before loading onto the array and imaged in media containing the applied stimuli. The array of wells was then washed with serum-free media and immediately applied onto a glass slide pre-coated with capture antibodies. After printing for 2 h, a solution of labeled antibodies—IL-17 (Alexa Fluor 488), IFNγ (Alexa Fluor 555), IL-2 (Alexa Fluor 594), TNFα (Alexa Fluor 700)—were used for detection.

Imaging and enumeration of cell-loaded arrays

All images were acquired on an automated inverted epifluorescence microscope (Zeiss) equipped for live-cell imaging (temperature and CO_2 control). The arrays were mounted face-up on the microscope with a coverslip placed on top of the array. Transmitted light and epifluoresence micrographs were collected block-by-block (7×7 microwells per block). The resulting collection of images was analyzed using a custom software program to determine the number of cells present in each well.

Primary cell retrieval and cloning

Memory T cells and monocytes were bead isolated using negative selection (Miltenyi Memory CD4+ T Cell Isolation Kit and Monocyte Isolation Kit II). Memory T cells and monocytes were combined in a 1:1 ratio in the presence of LPS (100 ng/mL) and anti-CD3 (OKT3 1 μg/mL) in HL-1 media and 10% fetal calf serum for 3 days before being deposited on the array of microwells and analyzed for IL-17 and IFN-γ secretion (2 h). The array of microwells was incubated in culture media supplemented with 20 U/mL IL-2 for 2 days after microengraving. Cells that exhibited IFNγ or IL-17 secretion in individual microwells were retrieved following a previously described protocol.[32, 37] Briefly, cytokine-secreting cells were retrieved from microwells using an automated system for micromanipulation (CellCelector, AVISO GmbH) equipped with a drawn glass capillary (50-μm diameter).[37] Retrieved cells were deposited into a round bottom 96-well microtiter plate containing irradiated PBMCs used as feeder cells for clonal expansion in the presence of PHA and IL-2. After two weeks, proliferated clones were collected, stimulated with PMA and ionomycin in the presence of monensin (BD GolgiStopT, BD Bioscience) and interrogated for cytokine expression by ICS.

Data analysis

The data extracted from both the array of cells and the matching printed microarrays were matched in Excel (Microsoft) using unique identifiers assigned to each well within the array. The dataset was filtered to include the locations in the array that contained only single cells matched to secreted proteins on the corresponding microarray for subsequent analysis in Excel or MATLAB (The Mathworks, Natick, MA). To convert the measured MFI for the cytokines captured from a given cell into a rate of secretion, we used a series of known amounts of fluorescent detection antibodies arrayed on a glass slide as a reference to translate MFI into a finite quantity of captured analyte (assuming a 1:1 relationship between the captured cytokine of interest and the detection antibody as rationalized below); dividing this number of molecules by the time of incubation yielded the average rate of secretion for a given cell. Box plots follow Tukey's convention, with the center line representing the median, and the upper and lower edges of the box representing the values of the upper and lower quartiles. Whiskers extending from each end of the box represent the most extreme values within 1.5 times the interquartile range.

Results and discussion

Modeling the capture of protein secreted from confined cells

To determine how secreted proteins distribute over time in the media surrounding a confined cell and onto the binding surface during microengraving, we executed a series of numerical simulations using our mathematical model for the diffusion and capture of proteins. These calculations suggested that the process involves three characteristic temporal regimes (Fig. 1b). Immediately after sealing the cell inside a well, the concentration of proteins in solution exceeds that present on the surface. After a short time (~30 min for a cell secreting 10 molecules/s), a steady–state distribution of protein is reached in solution, varying from a high concentration around the cell to a low concentration at the surface of the glass. (We note that this steady-state distribution is reached at approximately the same point in time regardless of the choice of the diffusion coefficient for the protein (10^{-9}–10^{-11} m^2/s).) In the ensuing period of time, the protein accumulates predominantly on the surface rather than in solution: The quantity of protein captured on the surface increases at a rate reflecting the rate of secretion from the cell ($dN_{surface}/dt \sim \kappa$), while the concentration of proteins in the media remains nearly constant. Eventually, the quantity of analytes on the surface approaches the total number of available binding sites on the surface ($C_s \sim \theta_0$). At this point (> 27 h), the rate of capture at the surface decreases, and the concentration of analytes in the media increases, rapidly approaching the total concentration of protein secreted.

Effects of system parameters on the capture of analytes

The simulations indicated that the intermediate temporal regime (t ~ 30 min to 27 h) represents the ideal period to measure the average rates of secretion for each cell in the array. The viability of mammalian cells in the sealed microwells, particularly primary cells, declines significantly after 4–6 h; this constraint establishes the practical upper bound on the length of time that is feasible for microengraving to less than 4 h.[28, 38] Within this range of times, we used our model to understand how the affinity (K_D) of the capture antibodies and the number of binding sites available on the surface (θ_0) may influence the quantity of analytes captured on the surface. The antibodies used to capture the secreted analytes should have high affinities (< 10 nM) (Fig. S2a). For an antibody with K_D~100 pM, the amount of protein captured on the surface closely approximates the total amount of protein secreted during the incubation ($N_{surface}$~95–99% N_{total}). We validated that the commercial antibodies used in this work to capture specific cytokines each have K_D~10–100 pM by ELISA measurements and data provided by the manufacturers.

The calculations also showed that increasing θ_0 improves the accuracy of the quantity captured (Fig. S2b). The optimal range calculated for θ_0 (~10^{-9}-10^{-8} mol/m^2) is consistent with the typical saturating densities measured for antibodies immobilized on hydrophilic surfaces (glass) from buffered solutions by optical reflectometry,[39, 40] surface plasmon resonance,[41] and spectroscopic ellipsometry,[42] and with our own measurements of the saturating quantity of antigen captured on the glass slides used here. For short times of incubation (30 min-4 h), the model suggested that the fraction of binding sites occupied with cytokines (κ=10 molecules/s) is less than 10%. This low occupancy makes it reasonable to assume that, under the typical experimental conditions employed for microengraving, the molar ratio of captured proteins to labeled monoclonal antibodies used for detection is approximately 1:1.

For a cell secreting at a constant rate, the model predicts the accumulated signal on the binding surface increases linearly with the rate of secretion. This trend implies that the total amount of analyte captured by microengraving for a given cell over a fixed period of time is a measure of its average rate of secretion. Simulations for the number of analytes accumulated on the surface after a fixed time (2 h) suggest that poor binding affinity for the capture antibody could lead to an underestimation of the absolute rates of secretion by approximately twofold (Fig. S2c). Together, these calculations imply that a relatively large range of operating parameters is possible without affecting the accuracy of the estimated rate by more than two- to threefold.

Geometric parameters, such as the size and shape of the well and even the position of a cell within the well, could also impact the diffusion and capture of the analytes. The design and fabrication of the microarray by replica molding determines the physical geometry of the wells, but the position of the cell in each well can vary. Through experimental observation, cells usually settle randomly on the bottom of each well, but they occasionally adhere to the sidewalls. Our model suggests that the position of the cell within the well influences the rate at which a steady-state distribution of analytes is reached in solution during the initial stages of the process, but that it does not affect the predicted range of times for the quantitative capture on the surface (Fig. S2d). This result implies that the location of the cell inside the well is not important, and that the signals detected from different wells across the same array are comparable. These results also indicate that changing the depth of the microwells within the same order of magnitude does not significantly alter the sensitivity of the assay, but changing the surface area exposed to the confined volume does. The initial rates of secretion and capture do not change with decreasing surface area, but the time to saturation decreases as the total number of binding sites decreases. Decreasing the exposed surface area (for a cell producing proteins at a constant rate) also increases the density of captured molecules on the surface (and therefore the total fluorescent signal measured). Therefore, for the same incubation time, the signal-to-noise ratio increases as the cross-sectional area of the wells decreases. These calculations suggest that the combination of cross-sectional area and incubation time will determine the upper and lower limits on the rates of secretion that can be determined accurately (Fig. S3). The steric crowding of cytokines and antibodies on the capture surface at high occupancy (~95% θ_0) establishes an upper bound on the rates detected, while the density of captured analytes will affect the lower limit of detection. For most cytokines (with rates of secretion typically <100 molecules/s), our model suggests the minimum time required for microengraving to detect 0.5 molecules/s is 1 h for 30 μm × 30 μm wells and 2 h for 50 μm × 50 μm wells. Taken together, the simulations discussed here indicate that a practical set of operating conditions for microengraving are possible wherein the rates of secretion for analytes such as cytokines can be detected down to 0.5 molecules/s within 1–2 h.

Experimental validation of predicted dynamics for capturing proteins by microengraving

Our model suggested that the amount of proteins from individual cells captured on a binding surface should increase monotonically with the time allowed for microengraving. To test this hypothesis, we measured the quantities of a cytokine (interleukin-6, IL-6) released from individual PBMCs after stimulation with a Toll-like receptor agonist, LPS, for 48 h. The median values of the MFI for IL-6 (captured from individual cells) increased linearly with time (Fig. 2a). This result matched the response predicted by the numerical simulations. The simulations also indicated that variations in intensities measured following a fixed period of time for microengraving should increase monotonically with increased rates of secretion. We used a mouse hybridoma cell line to measure the secretion of IgG by microengraving for three different periods of incubation, and plotted the median values of MFI as a function of the number of cells in each well (Fig. 2b). For each fixed period of microengraving, the quantity of captured IgG increased linearly with the number of cells in each well. These data establish that the variations in MFI of captured protein at a fixed time point reflect the variations in the amounts of protein secreted by individual cells, and, therefore, in the average rates of secretion per cell.

Determination of the rates of cytokine secretion from single cells

The linear relationship between the measured MFIs for captured proteins and the number of cells per well suggested that microengraving also could efficiently and quantitatively yield estimates for the amount of protein secreted from single cells within a defined period. We stimulated human PBMCs with LPS for 3, 6, and 12 h, and then captured IL-6 by microengraving. In parallel, we prepared a standard reference comprising known amounts of fluorescent detection antibodies (Fig. S4). Using this reference to convert the measured MFI for the captured cytokines into amounts, we determined the distribution in the individual rates of secretion for IL-6 among the population of cells (Fig. 3a). The limit of detection was defined as the rate of secretion corresponding to three standard deviations above the median MFI of the average background on the array. For IL-6, this limit was 0.6±0.1 molecules/s (when using 50 μm wells for microengraving with an incubation time of 2 h); the limits of detection determined for other cytokines were also similar (Table 2). This sensitivity exceeds that of antibody-based capture at the surfaces of secreting cells by nearly two orders of magnitude.[17] Based on the propagation of the uncertainties contributed both by approximations from our simulations and by the error of measurements in the experiment, we calculated that the uncertainty for the rate of secretion measured from a given cell is about 18%. The uncertainty of the measured area of individual elements on the microarray generated by microengraving (16%) was the dominant source of error because the spatial resolution of the scanner employed (5 μm) significantly limited the precision of this measure.

The measured responses showed that the frequency of IL-6-secreting cells (number of IL-6-secreting cells within the total population) increased with time, especially between 3 and 6h, and that the mean rate of secretion per cell increased monotonically from 6.5±3.2 (3 h) to 10.6±7.1 (12 h). This range of values is consistent with that estimated by ELISA (using the supernatents from the stimulated cells), and reported values in the literature for cytokine release from primary cells.[43] The expression of mRNA encoding *IL-6*, however, peaked at 6 h (Fig. 3b). This observation indicates, as expected, that the timing of transcription does not necessarily correlate with the timing for secretion of a protein. To assess whether the most productive cells were derived from a particular subset of cells within the PBMCs, the cells were labeled and then imaged *in situ* after microengraving. Most of the cells secreting IL-6 were $CD11b^{+}CD14^{-}$ (45%, 10±8.4 molecules/s) and $CD11b^{+}CD14^{+}$ (27%, 10±7.4 molecules/s), while a small population of cells were $CD3^{+}$ (4.7%, 12.5±9.4 molecules/s) (Fig. 3a insert and Table S1). Since CD11b and CD14 are markers predominantly associated

with monocytes, this result is consistent with previous reports that show LPS strongly mediates monocytes responses.[44, 45] The median rates of secretion for each class of cells, however, did not differ significantly (two-tailed, unpaired Student's t-test), suggesting the magnitudes of reponses to the applied stimulus of LPS for these different lineages of cells are all similar.

The combination of the frequency of responding cells and the distributions in their rates of secretion should facilitate distinguishing differences in the magnitude of functional immune responses after stimulation. We tested whether the distributions of rates of IL-6 secretion could differentiate responses between two individuals after exposing their PBMCs to three different stimuli. The responses of cells from the same donor exhibited strong variations in both frequency and magnitude (rates) depending on the stimulation, and this combination of responses was unique to the individuals (Fig. 3c). Both donors exhibited similar frequencies of responding cells when stimulated with PHA, but the distributions in the rates of secretion were quite different. Kolmogorov-Smirnov statistical tests of the distributions indicated that only two conditions of stimulation (LPS and PHA for Donor 2) were similar ($p=0.8622$). These results demonstrate that assays that distinguish immune responsiveness based on multiple, independent measures (frequencies and rates) may be more robust than those relying on single-parameter measures (frequencies).

Multiplexed detection of cytokines from single cells

The analysis of multiple cytokines concurrently is important for distinguishing different functional responses among lymphocytes, and for realizing robust clinical assays where samples are limited in size. We next extended the number of cytokines for which the rates of secretion could be analyzed simultaneously during microengraving. Our analytical model suggested that up to 10 individual antibodies within a mixed adsorbed layer could operate independently to capture different analytes from the same cell without affecting the individual limits of detection, assuming sufficient specificities for each pair of antibodies used for capture and detection. We tested commercial pairs of antibodies for IL-17, IFNγ, IL-2, and TNFα to determine a combination that exhibited no significant (< 3%) cross-reactivity at the maximum concentrations of cytokines relevant for microengraving (~10 ng/mL). To demonstrate the multiplexed analysis of cytokines by quantitative microengraving using this panel, we characterized the distributions in the rates of cytokines released from human PBMCs following stimulation with PMA and ionomycin. Representative images of viable single cells in microwells that produced up to three different cytokines within 2 h are shown in Fig. 4a. These results show that different cytokines can be detected simultaneously with this assay, and thus, the rates of secretion for each cytokine can be determined independently (Fig. 4b). We found that the release of IFNγ was the most dynamic (3.8–120 molecules/s), while the rates for other cytokines were typically less than 20 molecules/s. IFNγ and IL-2+ cells included both CD4 and CD8 T cells: Although the frequencies of each lineage differed, the distributions of their rates of secretion were similar (Fig. 4c). Together, these results show that multiple secreted factors can be scored quantitatively in parallel for individual cells within a heterogeneous population.

Retrieval of primary T cells for in vitro expansion

Microengraving is a sufficiently rapid and efficient process that individual cells remain viable, and can be retrieved afterwards from the microwells in which they are isolated.[28, 32] This characteristic implies that clonal lines of T cells or other primary lymphocytes could be generated on the basis of their functional profiles (e.g., secreted cytokines)—a criterion for selection of clones that is not possible by traditional ELISpot or ICS. To test whether primary T cell lines could be generated from their cytokine profiles determined by microengraving, we retrieved cells secreting either IL-17 or IFNγ from 50 μm wells after

microengraving and cultured them in 96-well microtiter plates containing irradiated PBMCs, PHA, and IL-2 to promote proliferation and expansion. After two weeks in culture, most of the retrieved cells had proliferated (>80 % efficiency). The cytokine profiles of these clones were then analyzed by ICS for IL-17 and IFNγ. After expansion, the majority of cells in each population still kept their original profiles of cytokine production; two examples are shown in Fig. 5. These results demonstrate that incubation of primary T cells in closed microwells for a short time (~2 h) does not change their viability, and that those cells can be specifically retrieved for expansion and for subsequent characterization by other analytical methods.

Conclusions

The quantitative extension to microengraving described here now makes it possible to categorize a population of viable lymphocytes on the basis of three independent attributes: 1) surface-expressed markers indicating their immunophenotypes, 2) the frequencies of cells secreting cytokines, and 3) the rates of secretion of those cytokines. Such multidimensional profiles of individual cells should improve the differentiation of heterogeneous subsets of cells that are crucial for evaluating vaccine responses and understanding the pathology of chronic diseases. The small volumes required for dispensing a population of cells onto an array of microwells makes the approach especially well-suited for detailed, quantitative characterization of clinical samples where the number of cells available may be insufficient for analysis by independent conventional methods (e.g., infants, tissue biopsies). The results from the analytical model, confirmed by experimental data, also emphasize a technical advantage associated with temporarily confining cells into small volumes that contain an appropriate capture reagent for one or more analytes of interest. In contrast to ELISpot, ELISA, and related adaptations of these conventional immunoassays implemented in open arrays of microwells,[18, 46] the non-equilibrium conditions for mass transport achieved by confining secreting cells significantly reduce the time required to detect specific analytes, and enhance the sensitivity of the assay to low quantities of released proteins. Finally, the ability to identify and recover cells of interest based on their functional attributes (e.g., profile of cytokine secretion) by quantitative microengraving provides a unique capability for further evaluating the heterogeneities among various clonotypes that is not possible by conventional ELISpot or ICS. Together, the combination of these characteristics suggests that quantitative, multiplexed microengraving should enable dynamic studies of the functional responses of individual primary lymphocytes following stimulation with new temporal resolution. Such measurements would allow detailed analyses of human lymphocytes that cannot be followed presently for individual cells—e.g., the plasticity of T cells and the timing of cytokine release from individual immune cells.

Supplementary Material

Refer to Web version on PubMed Central for supplementary material.

Acknowledgments

This research was supported in part by grants from the Deshpande Center for Technological Innovation, and the Dana Foundation. The project described was also supported in part by Award Numbers 5U19AI050864-07 (J.C.L.), F32AI651003 (E.M.B.), P01AI045757, U19AI046130, U19AI070352, and P01AI039671 (D.A.H.) from the National Institute of Allergy and Infectious Diseases. The content is solely the responsibility of the authors and does not necessarily represent the official views of the National Institute of Allergy and Infectious Diseases or the National Institutes of Health. D.A.H. is also supported by a Jacob Javits Merit Award (NS2427) from the National Institute of Neurological Disorders and Stroke. J.C.L. is a Texaco Mangelsdorf Career Development Professor.

References

1. Pantaleo G, Harari A. Nat Rev Immunol. 2006; 6:417–423. [PubMed: 16622477]
2. Seder RA, Darrah PA, Roederer M. Nat Rev Immunol. 2008; 8:247–258. [PubMed: 18323851]
3. Streeck H, Frahm N, Walker B. Nature Protocols. 2009; 4:461–469.
4. Gazagne A, Claret E, Wijdenes J, Yssel H, Bousquet F, Levy E, Vielh P, Scotte F, Goupil TL, Fridman WH, Tartour E. Journal of Immunological Methods. 2003; 283:91–98. [PubMed: 14659902]
5. Rebhahn JA, Bishop C, Divekar AA, Jiminez-Garcia K, Kobie JJ, Lee FEH, Maupin GM, Snyder-Cappione JE, Zaiss DM, Mosmann TR. Computer methods and programs in biomedicine. 2008; 92:54–65. [PubMed: 18644656]
6. Harriman WD, Collarini EJ, Cromer RG, Dutta A, Strandh M, Zhang F, Kauvar LM. Journal of Immunological Methods. 2009; 341:127–134. [PubMed: 19084532]
7. Henn AD, Rebhahn J, Brown MA, Murphy AJ, Coca MN, Hyrien O, Pellegrin T, Mosmann T, Zand MS. J Immunol. 2009; 183:3177–3187. [PubMed: 19675172]
8. Bromage E, Stephens R, Hassoun L. Journal of Immunological Methods. 2009; 346:75–79. [PubMed: 19465022]
9. Kannanganat S, Ibegbu C, Chennareddi L, Robinson HL, Amara RR. J Virol. 2007; 81:8468–8476. [PubMed: 17553885]
10. Darrah PA, Patel DT, De Luca PM, Lindsay RWB, Davey DF, Flynn BJ, Hoff ST, Andersen P, Reed SG, Morris SL, Roederer M, Seder RA. Nat Med. 2007; 13:843–850. [PubMed: 17558415]
11. Perfetto SP, Chattopadhyay PK, Roederer M. Nat Rev Immunol. 2004; 4:648–655. [PubMed: 15286731]
12. Tajiri K, Kishi H, Ozawa T, Sugiyama T, Muraguchi A. Cytometry A. 2009; 75:282–288. [PubMed: 19012320]
13. Kwak DJ, Augustine NH, Borges WG, Joyner JL, Green WF, Hill HR. Infect Immun. 2000; 68:320–327. [PubMed: 10603404]
14. Manz R, Assenmacher M, Pfluger E, Miltenyi S, Radbruch A. Proc Natl Acad Sci U S A. 1995; 92:1921–1925. [PubMed: 7892200]
15. Powell KT, Weaver JC. Biotechnology (N Y). 1990; 8:333–337. [PubMed: 1366534]
16. Turcanu V, Williams NA. Nat Med. 2001; 7:373–376. [PubMed: 11231640]
17. Frykman S, Srienc F. Biotechnol Bioeng. 1998; 59:214–226. [PubMed: 10099332]
18. Zhu H, Stybayeva G, Silangcruz J, Yan J, Ramanculov E, Dandekar S, George MD, Revzin A. Anal Chem. 2009; 81:8150–8156. [PubMed: 19739655]
19. Tokimitsu Y, Kishi H, Kondo S, Honda R, Tajiri K, Motoki K, Ozawa T, Kadowaki S, Obata T, Fujiki S, Tateno C, Takaishi H, Chayama K, Yoshizato K, Tamiya E, Sugiyama T, Muraguchi A. Cytometry. 2007; 71:1003–1010. [PubMed: 17972305]
20. Sasuga Y, Iwasawa T, Terada K, Oe Y, Sorimachi H, Ohara O, Harada Y. Anal Chem. 2008
21. Revzin A, Sekine K, Sin A, Tompkins RG, Toner M. Lab Chip. 2005; 5:30–37. [PubMed: 15616737]
22. Rettig J, Folch A. Anal Chem. 2005; 77:5628–5634. [PubMed: 16131075]
23. Ostuni E, Chen C, Ingber D, Whitesides G. Langmuir. 2001; 17:2828–2834.
24. Ochsner M, Dusseiller MR, Grandin HM, Luna-Morris S, Textor M, Vogel V, Smith ML. Lab Chip. 2007; 7:1074–1077. [PubMed: 17653351]
25. Kovac JR, Voldman J. Anal Chem. 2007; 79:9321–9330. [PubMed: 18004819]
26. Chin VI, Taupin P, Sanga S, Scheel J, Gage FH, Bhatia SN. Biotechnol Bioeng. 2004; 88:399–415. [PubMed: 15486946]
27. Park MC, Hur JY, Kwon KW, Park SH, Suh KY. Lab Chip. 2006; 6:988–994. [PubMed: 16874367]
28. Love JC, Ronan JL, Grotenbreg GM, van der Veen AG, Ploegh HL. Nat Biotechnol. 2006; 24:703–707. [PubMed: 16699501]

29. Bradshaw EM, Kent SC, Tripuraneni V, Orban T, Ploegh HL, Hafler DA, Love JC. Clin Immunol. 2008; 129:10–18. [PubMed: 18675591]
30. Ronan JL, Story CM, Papa E, Love JC. J Immunol Methods. 2009; 340:164–169. [PubMed: 19028499]
31. Song Q, Han Q, Bradshaw EM, Kent SC, Raddassi K, Nilsson B, Nepom GT, Hafler DA, Love JC. Anal Chem. 2010; 82:473–477. [PubMed: 20000848]
32. Ogunniyi AO, Story CM, Papa E, Guillen E, Love JC. Nat Protoc. 2009; 4:767–782. [PubMed: 19528952]
33. Bird JJ, Brown DR, Mullen AC, Moskowitz NH, Mahowald MA, Sider JR, Gajewski TF, Wang CR, Reiner SL. Immunity. 1998; 9:229–237. [PubMed: 9729043]
34. Gutenwik J, Nilsson B, Axelsson A. Biochem Eng J. 2004; 19:1–7.
35. Day YS, Baird CL, Rich RL, Myszka DG. Protein Sci. 2002; 11:1017–1025. [PubMed: 11967359]
36. Foote J, Eisen HN. Proc Natl Acad Sci U S A. 1995; 92:1254–1256. [PubMed: 7877964]
37. Choi JH, Ogunniyi AO, Du M, Kretschmann M, Eberhardt J, Love JC. Biotechnol Prog. 2010
38. Story CM, Papa E, Hu CC, Ronan JL, Herlihy K, Ploegh HL, Love JC. Proc Natl Acad Sci U S A. 2008; 105:17902–17907. [PubMed: 19004776]
39. Buijs J, vandenBerg PAW, Lichtenbelt JWT, Norde W, Lyklema J. Journal of Colloid and Interface Science. 1996; 178:594–605.
40. Buijs J, White D, Norde W. Colloid Surface B. 1997; 8:239–249.
41. Chen S, Liu L, Zhou J, Jiang S. LANGMUIR. 2003; 19:2859–2864.
42. Xu H, Lu JR, Williams DE. The Journal of Physical Chemistry B. 2006; 110:1907–1914. [PubMed: 16471762]
43. Otto NM, Schindler R, Lun A, Boenisch O, Frei U, Oppert M. Crit Care. 2008; 12:R107. [PubMed: 18710523]
44. Guha M, Mackman N. Cell Signal. 2001; 13:85–94. [PubMed: 11257452]
45. Davtyan TK, Harutyunyan VA, Hakobyan GS, Avetisyan SA. FEMS Immunol Med Microbiol. 2008; 52:370–378. [PubMed: 18294193]
46. Jin A, Ozawa T, Tajiri K, Obata T, Kondo S, Kinoshita K, Kadowaki S, Takahashi K, Sugiyama T, Kishi H, Muraguchi A. Nat Med. 2009; 15:1088–1092. [PubMed: 19684583]

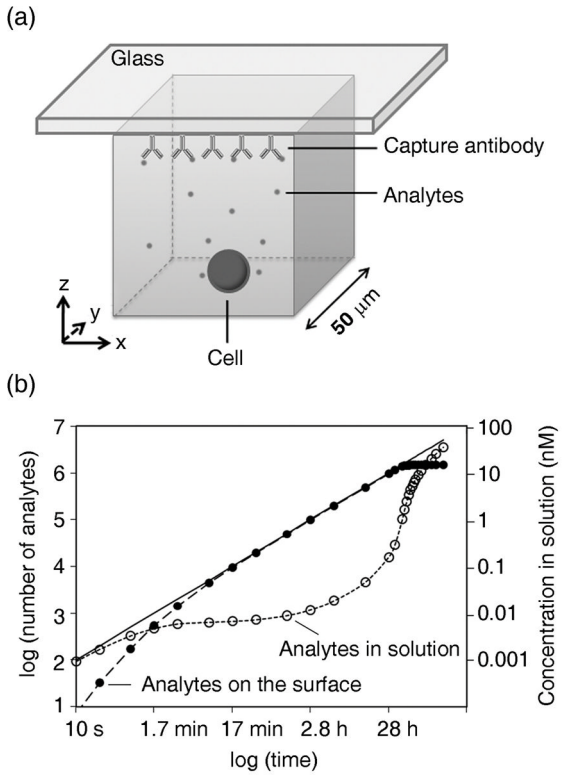

Figure 1.

Analysis of mass transfer and distribution of analytes during microengraving. (a) Schematic of the configuration of one microwell containing a single cell during microengraving. (b) Plot of the calculated quantity of analytes accumulated in the media (○) and on the surface of the glass (●) during microengraving when the cell secretes at a constant rate of 10 molecules/s. The solid line indicates the cumulative quantity of analytes secreted by the cell over time. For this simulation, the affinity of the capture antibody was K_D=100 pM, and the density of binding sites on the surface was $\theta_0=10^{-9}$ mol/m^2.

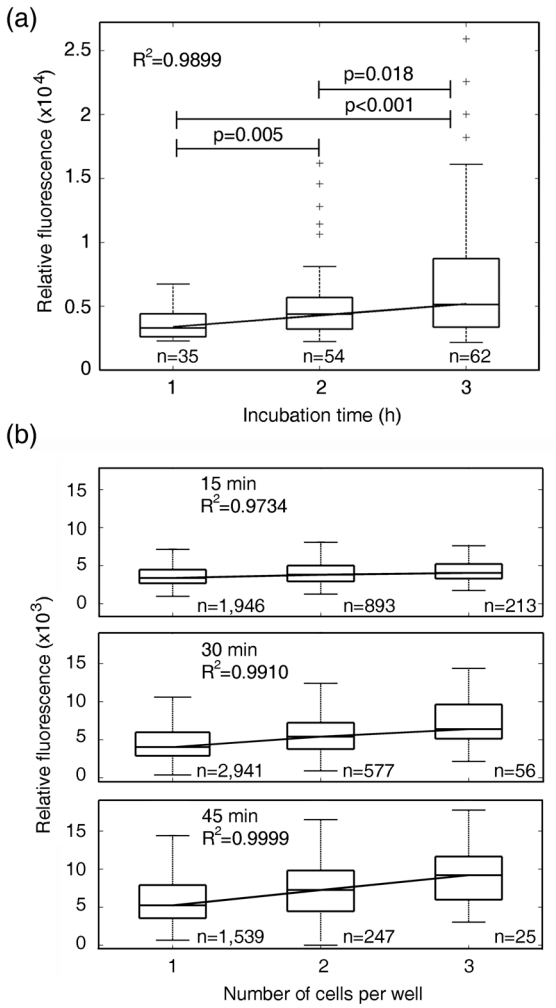

Figure 2.

Single-analyte measurements using microengraving. (a) Measurement of IL-6 secreted by individual human PBMCs. Boxplot of relative MFI of captured IL-6 as a function of incubation time. *n* is the number of events in each box. The solid line was fit by linear regression of the median values. Statistics were determined by a two-tailed Student's t-test. (b) Measurement of the secretion of antibodies from mouse hybridoma cells. The relative MFI of the signals were plotted as a function of the number of cells contained in each well for three different incubation times (15, 30, and 45 min). Solid lines were fit by linear regression. *n* is the number of events of each box.

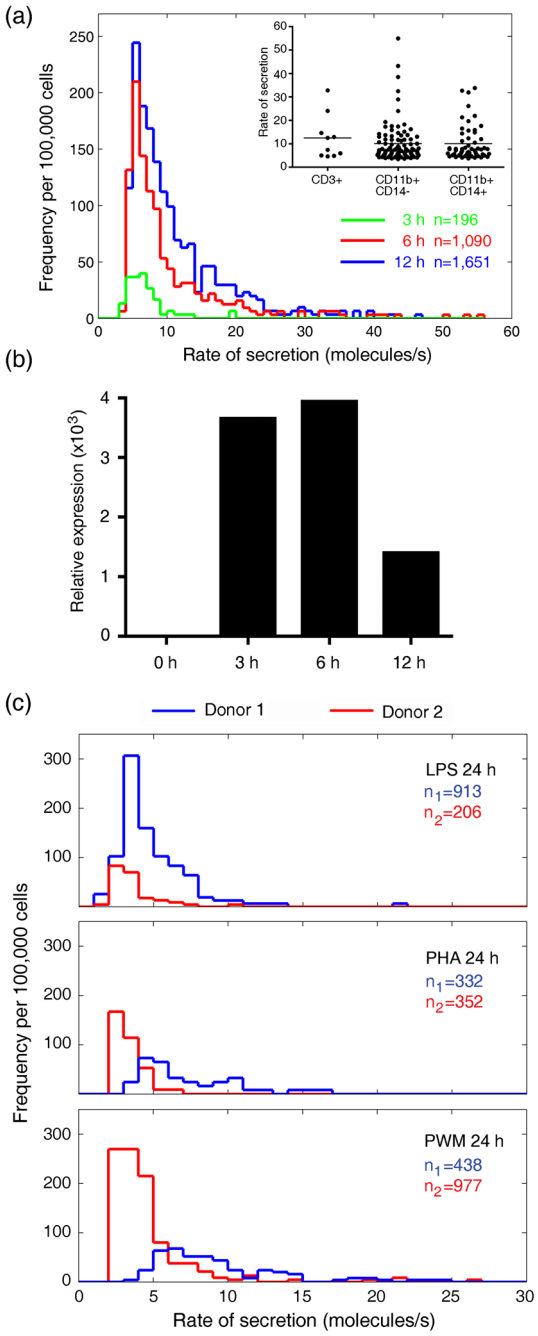

Figure 3.

Quantification of the frequencies and rates of secretion for single cells producing IL-6. (a,b) Production of IL-6 by human PBMCs following stimulation with LPS for 3, 6, or 12 h. (a) Histograms of the distribution of rates of secretion of IL-6 measured by microengraving (2 h) as a function of the time allowed for stimulation (3 h, green; 6 h, red; 12 h, blue). Insert: A plot of the specific rates of secretion determined for different subsets of cells within the array after 6 h stimulation. Horizontal bars indicate the mean value for each group. (b) mRNA levels of *IL-6* measured by quantitative PCR post-stimulation. (c) Histograms of the distribution of rates of secretion of IL-6 from PBMCs from two donors measured by microengraving (2 h) following stimulation with LPS, PHA or PWM for 24 h. The values *n*

indicated in (a) and (c) are the normalized frequencies of responding cells for each condition.

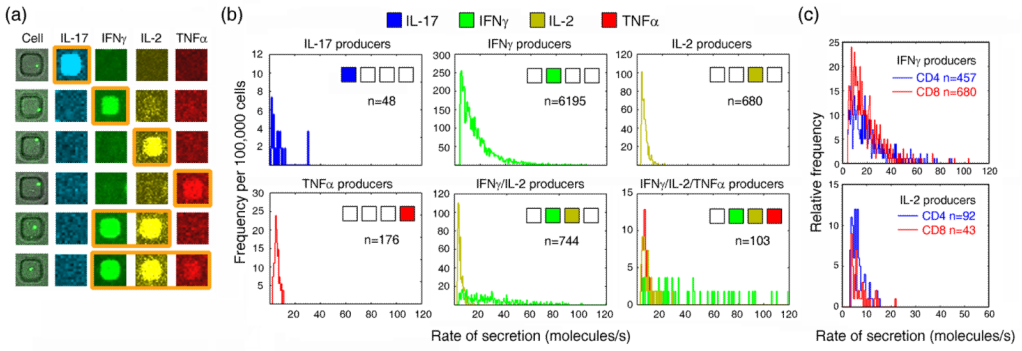

Figure 4.

Quadriplexed analysis of cytokines secreted from single cells. Human PBMCs were stimulated with PMA and ionomycin for 6 h, followed by microengraving for 2 h. (a) Representative images of individual cells in microwells matched with micrographs from the corresponding microarray of cytokines (arranged in rows). The first column shows composite micrographs of microwells (phase contrast) and viable cells (Calcein AM). The remaining four columns are micrographs extracted from the matching location on the printed microarray for each of four cytokines (IL-17, blue; IFNγ, green; IL-2, yellow; TNFα, red). Orange boxes outside the images indicate the positive spots in each row (MFI > background + 3SD). (b) Histograms of the calculated rates of secretion for each group of cytokine-producing cells. The colors are consistent with the assignments in (a). The inset rows of squares in each histogram indicate the combination of cytokines produced by the cells represented in the plot. The values of *n* indicated on each histogram are the normalized frequencies of cytokine-producing cells per 100,000 cells. The histograms were constructed with data from three independent experiments. (c) Histograms of the rates of secretion measured for CD4 and CD8 T cells producing IFNγ (top) or IL-2 (bottom). *n* is the number of cells imaged after microengraving bearing the indicated surface markers.

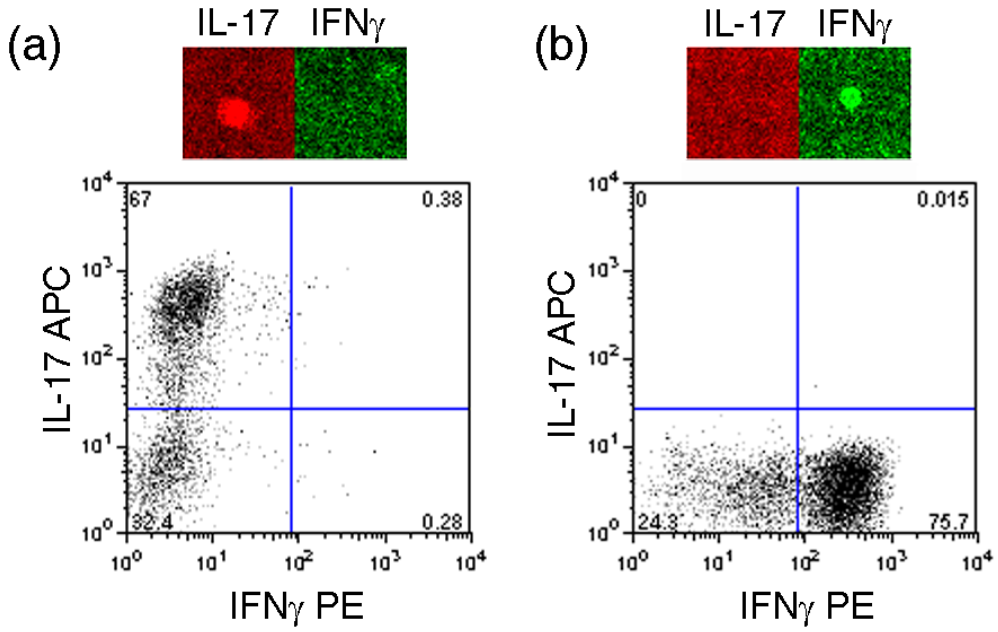

Figure 5.

Recovery and expansion of T cell lines selected by their cytokine profiles. T cells were stimulated with LPS-activated monocytes and anti-CD3 for 3 days, and then their cytokine profiles were determined by microengraving (2 h). The cells were cultured in the microwells for 48 h after microengraving, and then recovered by micromanipulation. The selected cells were expanded on irradiated PBMCs for 2 weeks, and then characterized by flow cytometry and intracellular staining. Fluorescent micrographs (top panels) indicate the cytokine profile measured by microengraving for (a) IL-17 secreting cells and (b) IFNγ-secreting cells. The number of cells present in both wells at the time of retrieval was four. The scatter plots (bottom panels) show the results of intracellular cytokine staining detected by flow cytometry. The expanded cells were stimulated with PMA/ionomycin in the presence of monensin, then fixed, permeabilized, and stained with antibodies against IFNγ (labeled with phycoerythrin (PE)) and IL-17 (labeled with allophycocyanin (APC)). Cytometry data were plotted in the graph according to the fluorescence intensities measured from both channels.

Table 1

Values of parameters used in simulation

Well size	50 μm×50 μm×50 μm
Cell diameter	10 μm
Diffusion coefficient (D)	10^{-10} m^2/s
Association rate constant (k_{on})	10^5–10^6 M^{-1} s^{-1}
Dissociation rate constant (k_{off})	10^{-3}–10^{-4} s^{-1}
Rate of secretion (κ)	1–100/cell/s
Density of total binding sites (θ_0)	10^{-8}–10^{-10} mol/m^2

Table 2

Experimental limits of detection for five cytokines

Cytokine	Fluorophore	Limit of detection (molecules/s)
IL-6	Alexa Fluor 488	0.5–0.7
IL-17	Alexa Fluor 488	0.5–0.6
IFNγ	Alexa Fluor 555	3.8–4.1
IL-2	Alexa Fluor 594	0.8–3.1
TNFα	Alexa Fluor 700	1.8–2.0

The limit of detection was determined for the specific fluorophore used on each detection antibody and defined as three standard deviations (SD) above the average background.